ORIGINAL RESEARCH

Diffusion Tensor Tractography-Based Group Mapping of the Pyramidal Tract in Relapsing-Remitting Multiple Sclerosis Patients

F. Lin
C. Yu
T. Jiang
K. Li
P. Chan

BACKGROUND AND PURPOSE: Many studies have reported abnormal changes in relapsing-remitting multiple sclerosis (RRMS) by histogram and region-of-interest–based methods by using diffusion tenor imaging. However, there are few studies on specific white matter fiber tracts of RRMS. Our study sought to use diffusion tensor tractography–based group mapping to investigate the presence of abnormal diffusion in the normal-appearing pyramidal tract (PYT) of RRMS and its possible mechanism.

METHODS: A PYT probability map was first constructed from data on 20 healthy patients based on the deterministic-based tractography method. The PYT probability map was then applied to 29 RRMS patients to calculate diffusion indices of the PYT. In this study, 4 quantitative indices—fractional anisotropy (FA), directionally averaged diffusion coefficient (D_{av}), axial diffusion coefficient (λ_1), and radial diffusion coefficient (λ_{23})—were used to characterize the abnormal diffusion.

RESULTS: Compared with healthy controls, RRMS patients had a significantly higher D_{av} and λ_{23} but a lower FA and a trend toward a lower λ_1 in the normal-appearing PYT. In RRMS patients, PYT lesions had a significantly higher λ_{23} and a lower FA, but there were no differences for D_{av} and λ_1 when compared with the normal-appearing PYT. Moreover, the diffusion indices derived from the normal-appearing PYT were significantly correlated with PYT lesion volumes by using the Spearman correlation analysis.

CONCLUSION: Our findings confirm the presence of abnormal diffusion in the normal-appearing PYT of RRMS patients and suggest that wallerian degeneration might be its mechanism.

Diffusion tensor imaging (DTI) is a noninvasive imaging technique capable of characterizing the diffusion properties of water molecules in vivo and detecting microstructural tissue changes not visible on conventional MR imaging.[1-3] Diffusion tensor, a 3×3 matrix, is introduced to model the motion of water molecules in brain tissue. Some quantitative rotationally invariant indices, which include fractional anisotropy (FA) and directionally averaged diffusion coefficient (D_{av}) derived from the diffusion tensor, can provide information about the magnitude and directionality of water diffusion and give clues on the microstructural properties of brain tissue.[4] Therefore, DTI is widely used in assessing many brain diseases, such as multiple sclerosis (MS), Alzheimer disease, and schizophrenia, and monitoring their treatments.[5-9]

Moreover, by tracking principal diffusion direction, the primary eigenvector of the diffusion tensor, diffusion tensor tractography can reconstruct major white matter fiber tracts, such as the corpus callosum, cingulum, and pyramidal tract (PYT).[10-12] Wilson et al and Lin et al used the tractography-based method to directly reconstruct the PYT of MS patients and quantified pathology related to specific impairment.[13,14] However, in MS patients, FA has been found to be extremely low in the normal-appearing white matter (NAWM), especially in the MS lesions,[6,7] which might result in the unreliable and erroneous termination of tractography. Taking this problem into account, some authors used the tractography-based group mapping method[15,16] to construct a white matter fiber tract probability map and then applied this map to normal subjects and patients to calculate diffusion indices inside the tract. Pagani et al used this kind of method to assess abnormal diffusion in the PYT of clinically isolated syndromes suggestive of MS patient.[17]

Although many studies have reported abnormal changes in MS by histogram and region-of-interest (ROI)–based methods by using DTI,[6,7,18] there are few studies on specific white matter fiber tracts of MS.[13,14,17] Some studies have reported that diffusion tensor eigenvalues can reflect specific pathologic or structural changes.[2,19,20] Diffusion tensor eigenvalues reflect the diffusion coefficients along the major, minor, and median axes of the diffusion ellipsoid. The axial diffusion coefficient (λ_1) reflects the diffusivity along the direction of maximum diffusion. The radial diffusion coefficient (λ_{23}), generated by averaging the last 2 eigenvalues due to their similarities in magnitude,[4] reflects the diffusivity orthogonal to the direction of maximum diffusion. Therefore, our study used the diffusion tensor tractography–based group mapping to investigate the presence of abnormal diffusion in the normal-appearing PYT of RRMS and its possible mechanism.

Methods

Subjects

Thirty patients with clinically definite RRMS were enrolled in this study between April 2003 and July 2005. To reduce possible influence of particular large lesion load, 29 RRMS patients were included in the

Received January 19, 2006; accepted after revision April 4.

From the National Laboratory of Pattern Recognition (F.L., T.J.), Institute of Automation, Chinese Academy of Sciences, Beijing, People's Republic of China; and the Departments of Radiology (C.Y., K.L.) and Neurology (P.C.), Xuanwu Hospital of Capital University of Medical Sciences, Beijing, People's Republic of China.

This work was partially supported by the Natural Science Foundation of China grant nos. 30425004, 30570509, 60121302, and 30470519, the National Key Basic Research and Development Program (973) grant no. 2004CB318107, and the Beijing Natural Science Foundation grant no. 7042026.

Address correspondence to Tianzi Jiang, PhD, National Laboratory of Pattern Recognition, Institute of Automation, Chinese Academy of Sciences, Beijing 100080, People's Republic of China; e-mail: jiangtz@nlpr.ia.ac.cn

final statistical analysis (18 women and 11 men; mean age = 32.8 ± 9.9 years, range = 18.0–55.0 years). The diagnosis of RRMS was based on the criteria proposed by Lublin and Reingold.[21] Their mean disease duration was 4.9 ± 4.8 years (range = 1.2–20.0 years), their mean Expanded Disability Status Scale (EDSS) score[22] was 2.8 ± 1.5 (range = 0.0–5.0), and their mean pyramidal functional system (PFS) score was 2.0 ± 1.3 (range = 0.0–4.0). Twenty sex- and age-matched healthy subjects (14 women and 6 men; mean age = 32.2 ± 10.6 years, range = 18.0–58.0 years) with no history of neurologic disorders and a normal neurologic examination were selected as control participants. When MR images were obtained, none of the patients was experiencing an acute relapse or being treated with corticosteroids or other drugs within 2 months. Local Ethical Committee approval and written informed consent from all the subjects were obtained before study initiation.

MR Data Acquisition

All MR imaging was performed on a 1.5T MR scanner (Sonata; Siemens, Erlangen, Germany). All sections were positioned to parallel a line that joins the most inferoanterior and inferoposterior parts of the corpus callosum.[23] The following sequences with identical axial section position, 30 sections, 4-mm section thickness, and 0.4-mm intersection gap were obtained 1) turbo spin-echo T2-weighted imaging (500/94/3 [TR/TE/NEX], 11 echo-train length, 256 × 224 matrix, 24 × 21-cm^2 FOV, in-plane resolution 0.47 × 0.47 mm from 0.94 × 0.94 mm after zero filling and 2) a single-shot, spin-echo, echo-planar pulse (EPI) imaging (5000/100/10, 128 × 112 matrix, and 24 × 21-cm^2 FOV, in-plane resolution 0.94 × 0.94 mm from 1.98 × 1.98 mm after zero filling). The diffusion-sensitizing gradients were applied along 6 noncollinear directions with a b value of 1000 s/mm^2, together with an acquisition without diffusion weighting ($b = 0$).

Data Analysis

The data were interpolated into isotropic voxels of 0.94 mm (matrix of 256 × 256 × 136), and the diffusion tensor for each voxel was derived according to the log-linear fitting algorithm.[24] After diagonalization of the diffusion tensor, 3 eigenvalues (λ_1, λ_2, λ_3) and their corresponding eigenvectors were obtained. Four quantitative indices including FA, D_{av}, λ_1, and λ_{23} were used to characterize the water diffusion in this study. These indices can be calculated by the following formula

$$1)\quad D_{av} = \frac{\lambda_1 + \lambda_2 + \lambda_3}{3},$$

$$\mathrm{FA} = \frac{\sqrt{(\lambda_1 - \lambda_2)^2 + (\lambda_1 - \lambda_3)^2 + (\lambda_2 - \lambda_3)^2}}{\sqrt{2(\lambda_1^2 + \lambda_2^2 + \lambda_3^2)}},\ \lambda_{23} = \frac{\lambda_2 + \lambda_3}{2}$$

Tractography-Based Group Mapping

Tractography is less reliable in MS patients than in healthy controls because FA is abnormally low in the NAWM, especially in MS lesions,[6,7] which may cause the erroneous termination of tractography. Therefore, we first constructed the PYT probability map from healthy volunteer data based on the multiple ROI deterministic tractography-based method,[11] and then applied this probability map to RRMS patients to calculate diffusion indices inside the PYT.

The PYT is known to be located in the middle third of the cerebral peduncle and the posterior limb of the internal capsule.[25-28] Thus, we manually delineated 2 ROIs on the axial planes. The first ROI was drawn on the middle third of the cerebral peduncle as seeding regions for tractography. The second ROI was drawn on the posterior limb of the internal capsule, as filtering regions to make sure that the reconstructed fibers were the PYT. All ROIs were drawn on the FA maps.

Diffusion tensor tractography was performed on DTI images employing the principal diffusion direction information based deterministic tracking algorithm by using the 4th-order Runge-Kutta method. First, each voxel in the first ROI was divided into 16 equal spaced starting seeds for tractography to reduce the partial volume effect. Then, tractography was performed by repeatedly following in small steps (0.3 mm) along the interpolated tensor field. Tractography was terminated if it made a turn of greater than 45° between 2 successive eigenvectors or if FA value of a voxel reached below 0.2.[25] The tracked fibers were filtered by the second ROI to make sure that the reconstructed tract was the PYT.

After the PYT was reconstructed, the diffusion-unweighted images of DTI ($b = 0$) were normalized to the standard Montreal Neurologic Institute (MNI) space by using an EPI template with statistical parameter mapping (SPM2; Wellcome Department of Imaging Neuroscience, London). The same transformation parameters were then applied to normalize the tracked PYT to the MNI space. After this, a PYT mask was created by calculating the voxels through which the PYT passed. Then, these masks for all healthy subjects were averaged to obtain the PYT probability map. The value of each voxel in map could be regarded as the probability that the voxel was part of the PYT.

Diffusion Indices of the PYT

The PYT probability map was used to calculate the weighted mean of the diffusion indices inside the PYT. The diffusion indices of the PYT were calculated as follows. First, the $b = 0$ image for each subject was normalized to the MNI space to obtain the transformation parameters. The transformation parameters were then applied to normalize the corresponding diffusion indices maps (FA, D_{av}, λ_1 and λ_{23}), and the PYT probability map was overlaid on these maps to calculate the weighted mean of the diffusion indices inside the PYT. For RRMS patients, it is necessary to analyze the diffusion prosperities in the PYT limited to lesions and the remaining normal-appearing PYT. To this end, lesions visible in the turbo spin-echo T2-weighted images were identified and manually extracted by an experienced radiologist with MRIcro (http://www.mricro.com). The lesions were also normalized to the MNI space to obtain the lesions distribution in the MNI space. Lesions were then used as masks to calculate the diffusion indices within the lesions and normal-appearing PYT. Moreover, lesion volume within the PYT for each RRMS patient was also obtained by using the PYT probability map.

Statistical Analysis

For the traced PYT, FA, D_{av}, λ_1, and λ_{23} were used as its characteristics. The group comparisons of these indices were performed with the Mann-Whitney U test because their distributions are non-Gaussian.[29,30] Correlations between these indices and EDSS scores or PFS scores or lesion volumes were assessed by the Spearman correlation analysis. A P value of less than .01 was considered statistically significant, and a value between .01 and .05 was considered a trend.[31]

Results

In this study, we concentrated our analysis on the portion of the PYT that includes the cerebral peduncle and the internal capsule, which are regions of high orientation coherence. Figure 1 illustrates this part of PYT probability map from data on healthy controls. The gray-scale indicates the probability of a voxel being part of the PYT.

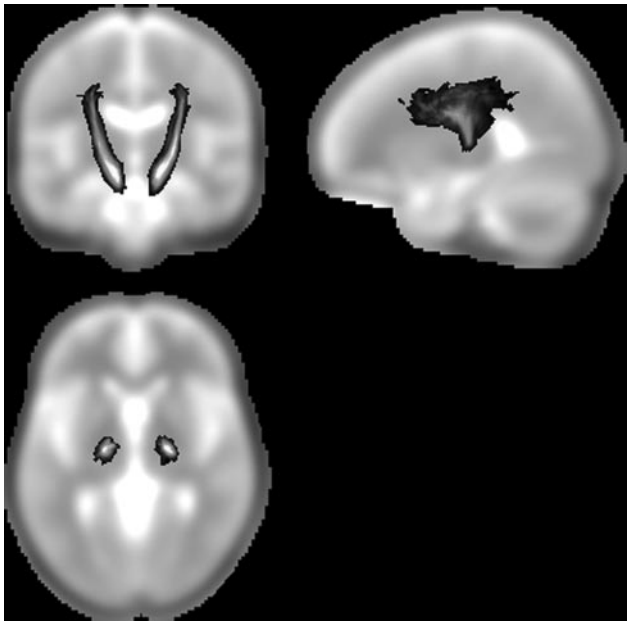

Fig 1. The pyramidal tract (PYT) probability map. The gray-scale overlay indicates the probability of a voxel being part of the PYT.

Compared with healthy controls, RRMS patients had a significantly higher D_{av} and λ_{23} and a lower FA, with a trend toward lower on λ_1 in the normal-appearing PYT ($P < .001$ for D_{av}; $P < .0001$ for λ_{23}; $P < .0001$ for FA; $P = .019$ for λ_1; Table). In RRMS patients, PYT lesions had a significantly higher λ_{23}, a lower FA, and no difference on D_{av} and λ_1 when compared with normal-appearing PYT ($P = .007$ for λ_{23}; $P < .0001$ for FA; $P = .051$ for λ_1; $P = .247$ for D_{av}; Table).

The PYT lesion volumes correlated well with the FA ($r = -0.512$, $P = .005$), D_{av} ($r = 0.548$, $P = .002$), λ_1 ($r = 0.529$, $P = .003$), and λ_{23} ($r = 0.542$, $P = .002$) all derived from the normal-appearing PYT (Fig 2).

Additionally, our method also required manually drawing 2 ROIs on sections. To test the reproducibility, 2 raters who were blind to the data drew these ROIs independently in 10 subjects randomly selected from the group of healthy subjects. The PYT probability map was constructed and the weighted mean of diffusion indices were calculated for the RRMS patients. Then intraclass correlation coefficients for inter-rater reliability were determined. For these indices, these coefficients ranged from 0.95 to 0.98.

Discussion

In this study, 4 indices derived from the diffusion tensor were used to investigate the presence of abnormal diffusion on the normal-appearing PYT of RRMS patients on the basis of a diffusion tensor tractography–based group mapping method.[15,16] Statistical analysis revealed that overall diffusivity and diffusion anisotropy of the normal-appearing PYT were significantly altered in RRMS patients.

In our study, we found that RRMS patients had a significantly higher D_{av} and λ_{23} and a lower FA, with a trend toward lower on λ_1 in the normal-appearing PYT when compared with normal controls (Table). These findings indicated that RRMS patients have abnormal diffusion in the normal-appearing PYT. The underlying pathologies may be axonal loss, decreases of axonal attenuation, increased extracellular space, and gliosis. Analysis of changes of diffusion tensor eigenvalues may provide more information about pathology. λ_1, which measures the diffusivity parallel to the main fiber direction, reflects the changes of restricted barriers along the direction of a fiber tract and the alterations of extracellular space. λ_{23}, which measures the diffusivity perpendicular to the main direction of fibers, reflects the changes of axonal membrane, myelin sheath, extracellular space, and so on.[2,29] Membrane disintegration and gliosis may create new diffusion barriers in the direction of a fiber tract and thus result in a decrease in diffusivity parallel to the main fiber direction and in reduced λ_1.[29,32,33] Loss of axonal structures may lead to the less restricted diffusion perpendicular to the main direction of fibers and to increased λ_{23}.[29,32,33] In combination, these effects are expected to lead to reduced FA and increased D_{av}.

The etiology of abnormal diffusion in the normal-appearing PYT for RRMS patients may be caused by wallerian degeneration. Recent studies have attempted to better delineate the diffusion changes associated with wallerian degeneration.[19,20] Pierpaoli et al[19] studied wallerian degeneration in the cortical spinal tract of patients with internal capsule lesions a year after stoke. Their results indicated reduced diffusion along the fibers (λ_1) and increased diffusion transverse to the fibers (λ_2 and λ_3; in our study, λ_{23}). Henry et al[20] examined the role of directional dependence of the apparent diffusion coefficients in the evaluation of normal-appearing brain regions of RRMS patients. They found reduced anisotropy and increased apparent diffusion coefficients with increased diffusion transverse to the fibers in regions with high anisotropy, such as the corpus callosum and internal capsule. They also attributed the pathology to wallerian degeneration.

The diffusion indices derived from the normal-appearing PYT correlated well with PYT lesion volumes (Fig 2), which further suggests that wallerian degeneration resulted in the abnormal diffusion in the PYT of our group of RRMS patients. Several previous studies have found some measurements of axonal attenuation correlated with lesion volumes and used these correlations as evidence for the predominance of wallerian degeneration.[17,34-36] Pagani et al[17] found that the diffusion indices from normal-appearing PYT correlated well with PYT lesion volumes in clinically isolated syndrome patients, and they concluded that these correlations reflected the presence of wallerian degeneration. Evangelou et al,[34] Ge et al,[35] and Oh et al[36] also found strong correlations between diffusion indices and lesion volumes and concluded that they reflected wallerian degeneration.

In our study, there were no correlations between any diffusion indices from the PYT and either EDSS or PFS score except that FA from the normal-appearing PYT showed a trend toward correlation with PFS scores. This might be because EDSS is a general scale that quantifies disability in 8 functional systems, whereas we concentrated only on the PYT for RRMS patients. Only FA from the normal-appearing PYT showed a trend toward correlation with PFS scores. This might be because of the low number of patients studied or it may also indicate that FA is more sensitive than other diffusion indices in monitoring treatment in RRMS patients.

There are several possible limitations in our study. First, due to the limitations of the streamline method for crossing fibers, especially at the level of the pons, the whole PYT cannot be consis-

Group comparisons of diffusion indices in the pyramidal tract (PYT) between the lowest section of the cerebral peduncle and the uppermost section of the lateral ventricle

		RRMS Patients		*P* Values	
	Controls	NA PYT	PYT Lesions	Controls Versus NA PYT	NA PYT Versus PYT Lesions
FA	0.46 ± 0.02	0.41 ± 0.04	0.34 ± 0.05	<.0001	<.0001
D_{av}	0.75 ± 0.02	0.85 ± 0.08	0.87 ± 0.09	<.0001	.247
λ_1	1.28 ± 0.03	1.25 ± 0.07	1.21 ± 0.10	.019	.051
λ_{23}	0.54 ± 0.02	0.65 ± 0.09	0.70 ± 0.10	<.0001	.007

Note:—RRMS indicates relapsing-remitting multiple sclerosis; NA, normal-appearing; FA, fractional anisotropy; D_{av}, directionally averaged diffusion coefficient ($\times 10^{-3}$ mm^2/s); λ_1, axial diffusion coefficient ($\times 10^{-3}$mm^2/s); λ_{23}, radial diffusion coefficient ($\times 10^{-3}$ mm^2/s). The group mean ± SD for the diffusion indices (Mann-Whitney *U* test) is reported in the second through fourth columns. A *P* value of <.01 is considered statistically significant, whereas a value between .01 and 0.05 is considered to represent a trend. The *P* values indicated that RRMS has abnormal diffusion in the normal-appearing PYT.

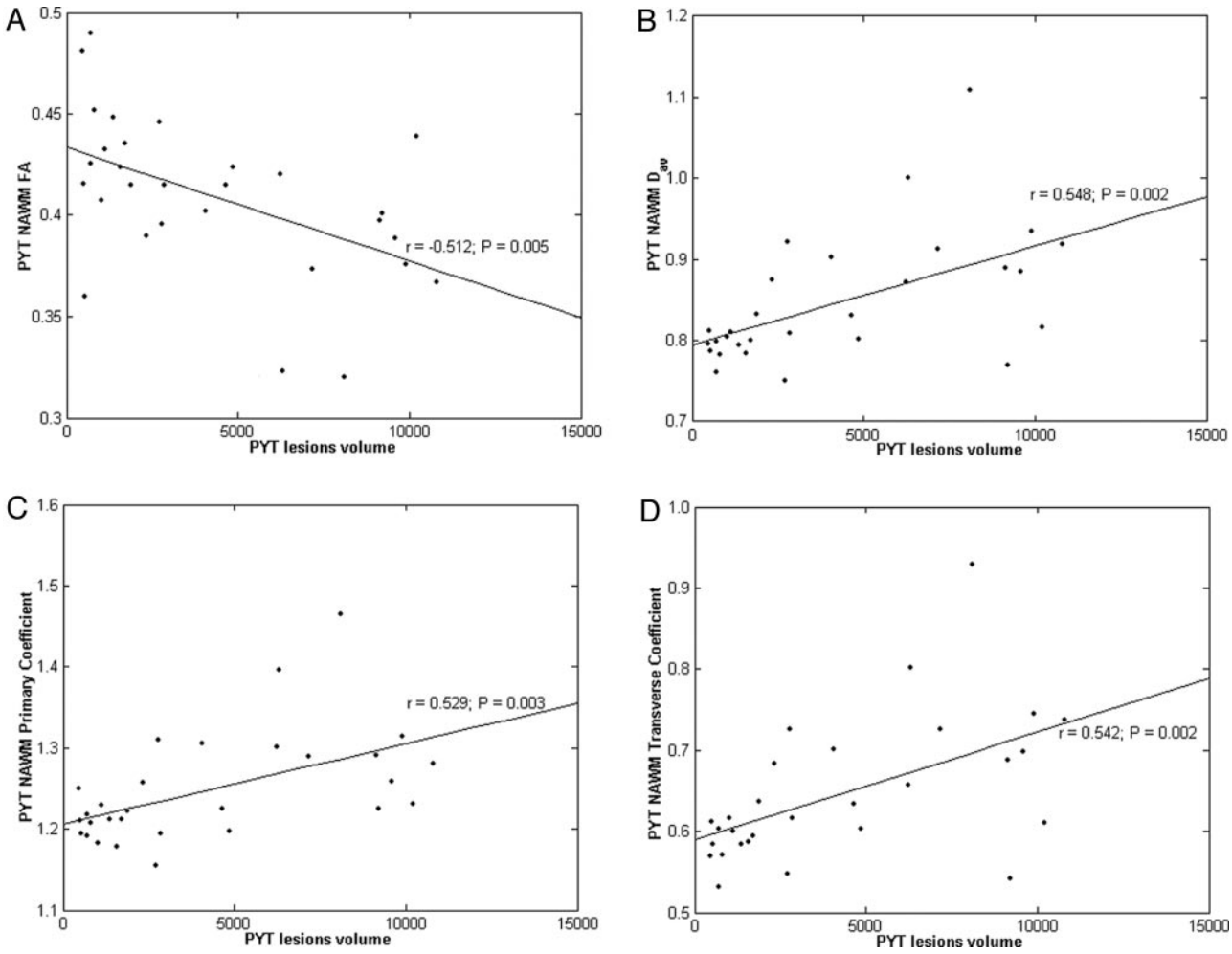

Fig 2. Correlation and scatter plots of diffusion indices derived from normal-appearing pyramidal tract (NA PYT) versus PYT lesion volumes. Scatter plots are shown of (*A*) fractional anisotropy (FA), (*B*) directionally averaged diffusion coefficient (D_{av}, × 10^{-3} mm^2/s), (*C*) axial diffusion coefficient (λ_1, × 10^{-3} mm^2/s), and (*D*) radial diffusion coefficient (λ_{23}, × 10^{-3} mm^2/s) versus PYT lesion volumes (mm^3).

tently traced for each subject. Improved tractography methods need to be developed to address this problem. Second, the poor resolution of the DTI sequences may have slightly influenced our measurements, and thus a higher resolution MR scanner may improve the reliability of diffusion measurements.

Conclusion

In this paper, diffusion tensor tractography–based group mapping was used to detect the abnormal diffusion in the normal-appearing PYT of RRMS patients. We found that RRMS patients had a significantly higher D_{av} and λ_{23} and a lower FA, as well as a trend toward lower λ_1 in the normal-appearing PYT when compared with normal controls, which might be caused by wallerian degeneration. In conclusion, this quantitative measurement approach of diffusion tensor tractography–based group mapping can detect subtle pathologic abnormalities beyond macroscopic lesions in white matter fiber tracts in MS; additionally, it can provide further anatomic insights into mechanisms of white matter damage and may also increase the specificity of DTI in the monitoring of specific neurologic deficits in MS. This method can also be used to investigate abnormal diffusion in other white matter fiber

tracts in a variety of neurologic conditions, including MS, stroke, cerebral tumors, dementia, and psychiatric disorders.

Acknowledgments

The authors are very grateful to the anonymous reviewers for their significant and constructive comments and suggestions, which greatly improved the article.

References

1. Basser PJ, Mattiello J, LeBihan D. **MR diffusion tensor spectroscopy and imaging.** *Biophys J* 1994;66:259–67
2. LeBihan D. **Looking into the functional architecture of the brain with diffusion MRI.** *Nat Rev Neurosci* 2003;4:469–80
3. LeBihan D, Mangin JF, Poupon C, et al. **Diffusion tensor imaging: concepts and applications.** *J Magn Reson Imaging* 2001;13:534–46
4. Basser PJ, Pierpaoli C. **Microstructural and physiological features of tissues elucidated by quantitative diffusion tensor MRI.** *J Magn Reson B* 1996;111: 209–19
5. Sundgren PC, Dong Q, Gomez-Hassan D, et al. **Diffusion tensor imaging of the brain: review of clinical applications.** *Neuroradiology* 2004;46:339–50
6. Filippi M, Cercignani M, Inglese M, et al. **Diffusion tensor magnetic resonance imaging in multiple sclerosis.** *Neurology* 2001;56:304–11
7. Griffin CM, Chard DT, Ciccarelli O, et al. **Diffusion tensor imaging in early relapsing-remitting multiple sclerosis.** *Mult Scler* 2001;7:290–7
8. Moseley M, Bammer R, Illes J. **Diffusion-tensor imaging of cognitive performance.** *Brain Cogn* 2002;50:396–413
9. Lim KO, Helpern JA. **Neuropsychiatric applications of DTI—a review.** *NMR Biomed* 2002;15:587–93
10. Basser PJ, Pajevic S, Pierpaoli C, et al. **In vivo fiber tractography using DT-MRI data.** *Magn Reson Med* 2000;44:625–32
11. Conturo TE, Lori NF, Cull TS, et al. **Tracking neuronal fiber pathways in the living human brain.** *Proc Natl Acad Sci USA* 1999;96:10422–27
12. Mori S, Crain BJ, Chacko VP, et al. **Three-dimensional tracking of axonal projections in the brain by magnetic resonance imaging.** *Ann Neurol* 1999;45:265–69
13. Wilson M, Tench CR, Morgan PS, et al. **Pyramidal tract mapping by diffusion tensor magnetic resonance imaging in multiple sclerosis: improving correlations with disability.** *J Neurol Neurosurg Psychiatry* 2003;74:203–07
14. Lin X, Tench CR, Morgan PS, et al. **'Importance sampling' in MS: use of diffusion tensor tractography to quantify pathology related to specific impairment.** *J Neurol Sci* 2005;237:13–19
15. Xu D, Mori S, Solaiyappan M, et al. **A framework for callosal fiber distribution analysis.** *Neuroimage* 2002;17:1131–43
16. Ciccarelli O, Toosy AT, Parker GJ, et al. **Diffusion tractography based group mapping of major white-matter pathways in the human brain.** *Neuroimage* 2003;19:1545–55
17. Pagani E, Filippi M, Rocca MA, et al. **A method for obtaining tract-specific diffusion tensor MRI measurements in the presence of disease: application to patients with clinically isolated syndromes suggestive of multiple sclerosis.** *Neuroimage* 2005;26:258–65
18. Cercignani M, Inglese M, Pagani E, et al. **Mean diffusivity and fractional anisotropy histograms of patients with multiple sclerosis.** *AJNR Am J Neuroradiol* 2001;22:952–58
19. Pierpaoli C, Barnett A, Pajevic S, et al. **Water diffusion changes in wallerian degeneration and their dependence on white matter architecture.** *Neuroimage* 2001;13:1174–85
20. Henry RG, Oh J, Nelson SJ, et al. **Directional diffusion in relapsing-remitting multiple sclerosis: a possible in vivo signature of wallerian degeneration.** *J Magn Reson Imaging* 2003;18:420–26
21. Lublin FD, Reingold RC. **Defining the clinical course of multiple sclerosis: results of an international survey.** *Neurology* 1996;46:907–11
22. Kurtzke JF. **Rating neurological impairment in multiple sclerosis: an expanded disability status scale (EDSS).** *Neurology* 1983;33:1444–52
23. Miller DH, Barkhof F, Berry I, et al. **Magnetic resonance imaging in monitoring the treatment of multiple sclerosis: concerted action guidelines.** *J Neurol Neurosurg Psichiatry* 1991;54:683–88
24. Basser PJ, Mattiello J, LeBihan D. **Estimation of the effective self-diffusion tensor from the NMR spin echo.** *J Magn Reson B* 1994;103:247–54
25. Kunimatsu A, Aoki S, Masutani Y, Abe O, et al. **The optimal trackability threshold of fractional anisotropy for diffusion tensor tractography of the corticospinal tract.** *Magn Reson Med Sci* 2004;3:11–17
26. Englander RN, Netsky MR, Adelman LS. **Location of human pyramidal tract in the internal capsule: anatomic evidence.** *Neurology* 1975;25:823–26
27. Glenn OA, Henry RG, Berman JI, et al. **DTI-based three-dimensional tractography detects differences in the pyramidal tracts of infants and children with congenital hemiparesis.** *J Magn Reson Imaging* 2003;18:641–48
28. Lee JS, Han MK, Kim SH, et al. **Fiber tracking by diffusion tensor imaging in corticospinal tract stroke: topographical correlation with clinical symptoms.** *Neuroimage* 2005;26:771–76
29. Pierpaoli C, Basser PJ. **Toward a quantitative assessment of diffusion anisotropy.** *Magn Reson Med* 1996;36:893–906
30. Pajevic S, Basser PJ. **Parametric and non-parametric statistical analysis of DT-MRI data.** *J Magn Reson* 2003;161:1–14
31. Nijeholt GJ, van Walderveen MA, Castelijns JA, et al. **Brain and spinal cord abnormalities in multiple sclerosis. Correlation between MRI parameters, clinical subtypes and symptoms.** *Brain* 1998;121:687–97
32. Thomalla G, Glauche V, Koch MA, et al. **Diffusion tensor imaging detects early Wallerian degeneration of the pyramidal tract after ischemic stroke.** *Neuroimage* 2004;22:1767–74
33. Kobayashi S, Hasegawa S, Maki T, et al. **Retrograde degeneration of the corticospinal tract associated with pontine infarction.** *J Neurol Sci* 2005;236:91–93
34. Evangelou N, Konz D, Esiri MM, et al. **Regional axonal loss in the corpus callosum correlates with cerebral white matter lesion volume and distribution in multiple sclerosis.** *Brain* 2000;123:1845–49
35. Ge Y, Law M, Johnson G, et al. **Preferential occult injury of corpus callosum in multiple sclerosis measured by diffusion tensor imaging.** *J Magn Reson Imaging* 2004;20:1–7
36. Oh J, Henry RG, Genain C, et al. **Mechanisms of normal appearing corpus callosum injury related to pericallosal T1 lesions in multiple sclerosis using directional diffusion tensor and 1H MRS imaging.** *J Neurol Neurosurg Psychiatry* 2004;75:1281–86